On the Development of a Modified Nonelectrolyte NRTL-NRF Model for Strong and Weak Electrolyte Solutions

Mazloumi, Seyed Hossein*⁺

Chemical Engineering Department, Faculty of Engineering, Ferdowsi University of Mashhad, Mashhad, I.R. IRAN

Shojaeian, Abolfazl

Department of Chemical Engineering, Hamedan University of Technology, Hamedan, I.R. IRAN

Haghtalab, Ali

Department of Chemical Engineering, Tarbiat Modares University, Tehran, I.R. IRAN

ABSTRACT: *The non-electrolyte NRTL-NRF model has been modified to study electrolyte solutions. The modified model for electrolytes is composed of short-range parts expressed by the modified nonelectrolyte NRTL-NRF and the Pitzer-Debye-Hückel equation to represent the long-range interactions of ions in the solution. In this work, a salt-specific parameter is used. Various types of experimental data including binary and ternary activity and osmotic coefficients, solid and gas solubilities in aqueous NaCl, and also aqueous Methyldiethanolamine (MDEA) data at wide temperature and pressure ranges have been implemented to check the performance of the present model. The overall relative standard deviation of 0.046 has been achieved for 130 strong aqueous binary electrolytes by the new model in fitting the experimental data of activity coefficients. The percent of absolute average deviations of the modified model for CO_2+ MDEA+ H_2O and H_2S+ MDEA+ H_2O are 30.3% and 24.8%, respectively. The results show the good capabilities of the model for electrolyte solutions.*

KEYWORDS: *Modified N-NRTL-NRF; Electrolyte; Activity; Osmotic; Aqueous MDEA.*

INTRODUCTION

Thermodynamic modeling of electrolyte solutions is a vital step in the design of various processes in chemical industries such as natural gas sweetening, desalination, and extraction [1, 2]. Modeling of electrolyte solutions is a complex subject due to the presence of ions with electrical charges that causes to form an unusual arrangement of species in the solution. The interactions of ions with the molecular species have to be taken in to an account to model the electrolyte properties. Also an electrostatic force, called a long-range force, between the ions must be considered. So the mathematical equations for thermodynamic modeling of electrolyte solutions can be noticeably complicated. Two different fundamental approaches have been adopted by various

investigators to study the electrolyte solutions. One of the method is the use of an equation of state (EOS) [3-10]. Using an electrolyte EOS, that is based on a residual Helmholtz energy function; various thermodynamic properties of electrolytes such as activity coefficient, solution density, solution enthalpy and etc. can be calculated. Another approach is to utilize an activity coefficient model that is based on a Gibbs free energy function. Although all thermophysical properties are not obtainable by this method directly, however it is an accurate and well-established method that has been already implemented for various theoretical and industrial studies [1]. Different theories such as the local composition concept have been used to develop activity coefficient models. Extension of the local composition concept for electrolyte solutions has been carried out by different approaches [11-35]. In the developments of a number of electrolyte models such as E-NRTL [12], E-Wilson [13], E-NRTL-NRF [14], E-Wilson-NRF [15], the assumptions of like-ion repulsion in local cell and local electroneutrality have been used. On the other hand, some investigators [20-25, 27-29] have been directly used nonelectrolyte, local composition models such as nonelectrolyte UINQUAC, NRTL-NRF, Wilson-NRF, and UNIQUAC-NRF using a number of assumptions such as ion-pair assumption and large values for like-ion repulsion interaction energy parameters in local cells.

The key difference between the mentioned electrolyte local composition models is in the type of interaction energy in local cells (enthalpic, Gibbs energy, or internal energy form) or (and) in reference states for neutral and ionic central cells. For example, the main difference between the E-Wilson [13] model and the E-NRTL [12] model is the assumption that the short-range energy parameter between species in a local cell has an enthalpic form rather than a Gibbs energy form. Also, the main difference in the derivation of E-NRTL [12] and E-NRTL-NRF [14] is in their reference states of local cells. In the later model, the case of random cells is adopted for the reference states however in the former one the pure and completely dissociated electrolytes are assumed.

In foregoing works, the nonelectrolyte NRTL-NRF [22, 28], nonelectrolyte Wilson-NRF [21, 27], and nonelectrolyte UNIQUAC-NRF [29] have been extended for electrolyte solutions by ion-pair and also large values for like-ion repulsion interaction energy assumptions. The results of these models are in very good agreement with electrolyte experimental data, however, these models are not reduced to the original nonelectrolyte NRTL [36], Wilson [37], and UNIQUAC [38] models in the absence of ions. The plan of this work is to modify the N-NRTL-NRF in such a way that not only the modified model has the strength to represent electrolyte properties with good accuracy, but also to reduce to the nonelectrolyte NRTL model [36] in the absence of ions. In view of the fact that the modified model originates on the nonelectrolyte framework, it has a simple form. Therefore, the aim of this study is to develop a modified nonelectrolyte NRTL-NRF model for electrolyte solutions with three main features; simplicity, accuracy, and reduction to nonelectrolyte NRTL [36] model in the absence of ions.

THEORETICAL SECTION
The modified thermodynamic model

As mentioned, the nonelectrolyte NRTL-NRF for electrolyte solutions [22, 28] does not reduce to NRTL [36] model in the absence of ions. In the development of nonelectrolyte NRTL-NRF, the reference state of all local cells, solvent, and ion, are random state of solutions, however, if one considers the pure state as the reference state for solvent and a random state for ions, then the modified nonelectrolyte model would reduce to the NRTL [36] model in the absence of ions. So, based on the two-liquid theory for nonelectrolytes [1], the derivation of the modified model in term of excess Gibbs free energy for a binary solution is as follows

$$g^E = x_1 g_I^E + x_2 g_{II}^E = x_{11}g_{11} + x_{21}g_{21} - \tag{1}$$
$$g_I^{Ref} + x_{12}g_{12} + x_{22}g_{22} - g_{II}^{Ref}$$

Where superscripts *E* and *Ref* denote excess and reference sate, respectively. Subscript I stands for a local cell in which component 1 (solvent) is the central molecule and similarly the subscript II stands for local cell with central molecule of component 2 (ion). x_{ij} is the local mole fraction of component *i* in cell with central molecule of component *j*. The reference states are

$$g_I^{Ref} = g_1 \tag{2}$$

$$g_{II}^{Ref} = x_1 g_{12} + x_2 g_{22} \tag{3}$$

Using the Eqs. (1-3) and definition of local mole fraction ($x_{ij} = x_i \Gamma_{ij}$), one can obtain the modified excess Gibbs energy model for binary solutions as:

$$\frac{g^E}{RT} = x_1 x_2 \left[\tau_{12} \left(\Gamma_{12} - 1 \right) + \tau_{21} \Gamma_{21} \right] \tag{4}$$

$$\Gamma_{ij} = \frac{G_{ij}}{\sum\limits_{l=1}^{n} x_1 G_{ij}} \tag{5}$$

$$G_{ij} = \exp\left(-\alpha_{ij} \frac{g_{ij} - g_{jj}}{RT} \right) = \exp\left(-\alpha_{ij} \tau_{ij} \right) \tag{6}$$

Where n is the number of components and α is non-randomness coefficient. The activity coefficient of components can be obtained by proper derivation of Eq.(4) $\left(\ln \gamma_i = \left[\partial (n_t g^E / RT) / \partial n_i \right]_{T,P,n_{j \ne i}} \right)$ as

$$\ln \gamma_1 = x_2^2 \left(\tau_{21} \Gamma_{21}^2 + \frac{\tau_{12} \Gamma_{12}^2}{G_{12}} - \tau_{21} \right) \tag{7}$$

$$\ln \gamma_2 = x_1^2 \left(\tau_{12} \Gamma_{12}^2 + \frac{\tau_{21} \Gamma_{21}^2}{G_{21}} - \tau_{12} \right) \tag{8}$$

The Eqs. (7) and (8) are the new modified activity coefficients model for binary systems. So, in this work, we have proposed a new non-electrolyte equation for electrolyte solution based on local composition with Gibbs interaction energy in local cells. The novelty of the work is in the adoption of reference state as that of local cells in a nonelectrolyte framework. Adoption of pure water as the reference state for water is more logical than the random state whereas the state of pure ion is an unreal state compared to the random state of ion which seems to be more logical. Generalizations of the Equations (6-8) for multi-component systems are:

$$\frac{g^E}{RT} = \sum_i x_i \left[\sum_j x_j \Gamma_{ij} \tau_{ij} - \sum_{\substack{l = \text{ion} \\ \text{pair or ion}}} x_1 \tau_{il} \right] \tag{9}$$

$$\ln \gamma_{i=\text{solvent}} = \sum_j x_j \left[\Gamma_{ji} \tau_{ji} + \Gamma_{ij} \left(\tau_{ij} - \sum_r x_r \tau_{rj} \Gamma_{rj} \right) \right] - \tag{10}$$

$$\sum_{\substack{l = \text{ion} \\ \text{pair or ion}}} x_1 \left[\tau_{il} - \sum_p x_p \tau_{pl} \right]$$

$$\ln \gamma_{i=\text{ion or ion pair}} = \sum_j x_j \left[\Gamma_{ji} \tau_{ji} + \right. \tag{11}$$

$$\left. \Gamma_{ij} \left(\tau_{ij} - \sum_r x_r \tau_{rj} \Gamma_{rj} \right) - \tau_{ij} \right] - \sum_{\substack{l = \text{ion} \\ \text{pair or ion}}} x_1 \left[\tau_{il} - \sum_p x_p \tau_{pl} \right]$$

As one can see in the equations (9), the third summation stand for ion, so in the absence of ion in the solution, this term vanishes, and the NRTL [36] model $\left(g^E / RT = \sum_i x_i \sum_j x_j \Gamma_{ij} \tau_{ij} \right)$ is recovered. It also arises for the activity coefficient of solvent (Eq. (10)). By omitting the two last summations in equation (10), the activity coefficient of NRTL is recovered $\left(\ln \gamma_i^{NRTL} = \sum_j x_j [\Gamma_{ji} \tau_{ji} + \Gamma_{ij} (\tau_{ij} - \sum_r x_r \tau_{rj} \Gamma_{rj})] \right.$.)

Application of the modified model for electrolytes

The activity coefficients of species in the electrolyte solution, based on excess Gibbs free energy formalism, is usually composed of two terms, one for short-range contribution and one for long-range contribution of ions. The long-range contribution of ion and water activity coefficient in electrolyte solutions is calculated using the Pitzer-Debye-Hückel as

$$\ln \gamma_{ion,LR}^* = -A \left(\frac{1000}{M_w} \right)^{0.5} \left(\frac{2 z_{ion}^2}{\rho} \ln \left(1 + \rho I_x^{1/2} \right) + \tag{12} \right.$$

$$\left. \frac{z_{ion}^2 I_x^{1/2} - 2 I_x^{3/2}}{1 + \rho I_x^{1/2}} \right)$$

$$\ln \gamma_{w,LR} = -A_\phi \left(\frac{1000}{M_w} \right)^{0.5} \left(\frac{2 I_x^{1.5}}{1 + \rho I_x^{0.5}} \right) \tag{13}$$

$$I_x = 0.5 \sum_{ion} x_{ion} z_{ion}^2 \tag{14}$$

Where A_ϕ is the Debye–Hückel constant, ρ is the closest ion approach, subscript w denotes water, M_w is the molecular weight of solvent, z is the charge number of ionic species, and x_{ion} is the mole fraction of cation or anion. For short-range contributions, the modified model is used.

In this work, a solution of an aqueous strong electrolyte such as aqueous KCl, is considered as a binary solution; water component 1 and KCl component 2. The mean activity coefficient of the electrolyte, e.g. KCl, is assumed as an ion pair and is computed as

$$\ln \gamma_2^* = \left(\ln \gamma_\pm \right) = \left(\ln \gamma_2 \right)_{LR}^* + \left(\ln \gamma_2 \right)_{SR}^* \tag{15}$$

Where $\pm$ denotes the mean activity coefficient of the electrolyte. The unsymmetrical short-range activity coefficient of the electrolyte using the modified model (Eq. (8)) is

$$\left(\ln \gamma_2 \right)^*_{SR} = \left(\ln \gamma_{\pm} \right)_{SR} = \ln \gamma_2 - \left(\ln \gamma_2 \right)^{\infty} = \tag{16}$$

$$x_1^2 \left(\tau_{12} \Gamma_{12}^2 + \frac{\tau_{21} \Gamma_{21}^2}{G_{21}} - \tau_{12} \right) - \tau_{21} G_{21}$$

Where ∞ denotes the infinite dilution state (i.e. x_2 approaches to zero). Also

$$\left(\ln \gamma_2 \right)^*_{LR} = \left(\ln \gamma_{\pm} \right)^*_{LR} = \frac{\nu_a \left(\ln \gamma_a \right)^*_{LR} + \nu_c \left(\ln \gamma_c \right)^*_{LR}}{\nu} \tag{17}$$

Where ν_a and ν_c are, respectively, anion and cation stoichiometric number and $\nu = \nu_a + \nu_c$. The anion and cation long-range activity coefficients, $\left(\ln \gamma_a \right)^*_{LR}$ and $\left(\ln \gamma_c \right)^*_{LR}$ are calculated using Eq. (12). The osmotic coefficient and the water activity coefficient in the electrolyte solutions can be calculated as

$$\Phi = - \frac{\ln \left(x_w \gamma_w \right)}{m \nu M_w} \tag{18}$$

$$\ln \gamma_w = \ln \gamma_1 = \left(\ln \gamma_w \right)_{LR} + \left(\ln \gamma_w \right)_{SR} \tag{19}$$

Where $\left(\ln \gamma_w \right)_{LR}$ and $\left(\ln \gamma_w \right)_{SR}$ are calculated using Eqs. (13) and (7), respectively.

RESULTS AND DISCUSSION
Strong aqueous binary electrolyte

In this section, the new model is applied for the representation of the mean activity coefficient of aqueous strong electrolyte solutions using the salt parameter approach. To do this, a wide variety of aqueous strong electrolyte solutions, more than 130 electrolytes, have been selected and listed in Table 1. In the calculations, the values of 0.125, 0.390947, and 14.9 have been adopted for the non-randomness factor α, the Pitzer-Debye-Hückel constant A_{φ}, and the parameter ρ, respectively. It should be noted that in this approach the mole fractions of species are calculated as $x_1 = x_{water} = 55.51/(55.51 + \nu m)$, $x_{salt} = x_2 = 1 - x_1$, $x_c = x_2 \nu_c / \nu$ and $x_a = x_2 \nu_a / \nu$. Since in this approach the binary aqueous electrolyte solution is considered as a binary solution so the new equation has two adjustable parameters

per each electrolyte, τ_{12} and τ_{21}. The parameters can be obtained by correlation of the experimental data of molality-based activity coefficient (γ_1^m). Thus, the mole fraction based activity coefficient (γ_1^x), obtained by the modified model Eq. (15), must be converted to the molality-based activity coefficient ($\gamma_1^m = x_w \gamma_1^x$). The adjusted parameters of the new model for 131 aqueous electrolytes are reported in Table 1. It can be seen from Table 1 that the overall relative standard deviations of 0.0198, 0.0166, 0.0778, 0.0584, and 0.0638 have been respectively achieved for uni-univalent, uni-divalent, di-univalent, di-divalent and tri-univalent electrolytes by the new model in fitting the experimental data of activity coefficients [39, 40]. Also included in Table 1 are the comparisons of the results of the new model with E-NRTL [12], E-NRTL-NRF [13], and Nonelectrolyte Wilson-NRF (NWN) [21]. It should be noted that the relative standard deviations of the E-NRTL for 1:1 electrolyte, reported in Table 1, have been obtained based on fitting of the experimental activity coefficient data of *Hamer* and *Wu* [27]. One can see the results of the new model for correlations of the activity coefficients (based on overall deviations) are better than E-NRTL especially for electrolytes with highly positive deviation at high molalities such as HCl, HBr, and NaOH. It can be observed that the results of the new model for correlations of the activity coefficients are as well, and in some electrolytes better than E-NRTL-NRF [13]. In addition, the results, in terms of overall deviations, are more accurate (except in 1:1 electrolytes) than the NWN model. It is remarkable neither the E-NRTL-NRF reduces to original NRTL [36] model in the absence of ions and nor the NWN to the original Wilson [37] model. Given in Table 1 is also the results of the new model in predicting osmotic coefficient data of 131 electrolytes. The overall relative standard deviations of the new model for calculation of osmotic coefficients are 0.0238, 0.0191, 0.0953, 0.130, and 0.0526 for uni-univalent, uni-divalent, di-univalent, di-divalent and tri-univalent electrolytes, respectively. Figs. 1-3 show the comparisons of the results of the new model with the experimental data at 298 K. As shown in Fig. 1, the agreements of the results of the new model with the experimental data are very good even at high molalities. Fig. 2 shows the prediction capability of the new model in predicting osmotic coefficients of some uni-univalent

Table 1: The fitted parameters of the present model based on salt specific parameter approach and the relative standard deviation* of the present model and the E-NRTL-NRF and NWN [15] in correlating of the experimental activity coefficient and the prediction results of the present model in representing of experimental osmotic coefficient at 298 K. The uni-univalent experimental data were taken from [39] and the others from [40].

electrolyte Uni-Univalent	max. m	τ_{21}	τ_{12}	$\delta\gamma_\pm$ This work	δ_Φ This work	$\delta\gamma_\pm$ E-NRTL	$\delta\gamma_\pm$ E-NRTL-NRF	$\delta\gamma_\pm$ NWN
AgNO3	15	12.711	4.418	0.0149	0.0237	0.014	0.014	0.027
CsAc	3.5	-3.463	-5.523	0.0053	0.0041	0.005	0.008	0.006
CsBr	5	-2.132	5.015	0.0074	0.0070	0.005	0.005	0.007
CsCl	11	-1.772	4.257	0.0158	0.0126	0.006	0.013	0.013
CsI	3	-2.000	4.971	0.0076	0.0078	0.007	0.005	0.008
CsNO3	1.5	-2.646	7.165	0.0022	0.0026	0.002	0.000	0.002
HBr	11	-5.558	8.984	0.0740	0.0323	0.183	0.040	0.052
HCl	16	-4.895	7.883	0.0575	0.0258	0.198	0.024	0.042
HClO4	10	-5.479	9.031	0.0923	0.0403	0.182	0.060	0.073
HI	10	-5.627	8.812	0.0899	0.0375	0.180	0.062	0.071
HNO3	28	-2.575	2.893	0.0195	0.0126	0.024	0.018	0.018
Kac	3.5	-3.029	-3.728	0.0063	0.0051	0.006	0.008	0.007
KBr	5.5	-1.784	3.031	0.0136	0.0020	0.014	0.004	0.014
KCl	5	-1.827	3.431	0.0019	0.0018	0.004	0.021	0.002
KCNS	5	-2.772	-7.427	0.0013	0.0012	0.002	0.003	0.002
KF	6	-3.028	5.167	0.0055	0.0043	0.012	0.006	0.006
KH adipate	1	-0.997	0.000	0.0021	0.0023	0.002	0.003	0.002
KH malonate	5	-0.752	3.376	0.0033	0.0038	0.003	0.004	0.003
KH succinate	4.5	-1.687	4.184	0.0018	0.0018	0.002	0.003	0.002
KH2PO4	1.8	-2.463	6.984	0.0044	0.0053	0.004	0.002	0.004
KI	4.5	-3.146	-7.626	0.0026	0.0023	0.003	0.005	0.003
KNO3	3.5	-0.387	4.897	0.0067	0.0076	0.006	0.004	0.007
KOH	20	-4.737	8.064	0.0831	0.0382	0.274	0.039	0.065
LiAc	4	-2.417	2.960	0.0034	0.0027	0.003	0.005	0.003
LiBr	6	-4.820	7.537	0.0206	0.0119	0.041	0.045	0.018
LiCl	19.219	-4.939	8.248	0.0659	0.0333	0.266	0.052	0.049
LiClO4	4.5	-4.281	5.705	0.0162	0.0107	0.022	0.017	0.016
LiI	3	-3.868	4.211	0.0188	0.0137	0.019	0.020	0.019
LiNO3	20	-3.241	4.496	0.0149	0.0085	0.039	0.016	0.014
LiOH	5	-2.843	6.202	0.0231	0.0249	0.020	0.021	0.022
LiTol	4.5	-2.902	-7.562	0.0121	0.0117	0.013	0.014	0.013

Table 1: The fitted parameters of the present model based on salt specific parameter approach and the relative standard deviation* of the present model and the E-NRTL-NRF and NWN [15] in correlating of the experimental activity coefficient and the prediction results of the present model in representing of experimental osmotic coefficient at 298 K. The uni-univalent experimental data were taken from [39] and the others from [40]. (Continued)

electrolyte	max. m	τ_{21}	τ_{12}	$\delta\gamma_{\pm}$	δ_{Φ}	$\delta\gamma_{\pm}$	$\delta\gamma_{\pm}$	$\delta\gamma_{\pm}$
NaBr	9	-3.383	5.468	0.0124	0.0078	0.032	0.061	0.012
NaBrO3	2.617	-1.043	3.804	0.0006	0.0166	0.001	0.002	0.001
Na butyrate	3.5	-4.787	-11.538	0.0065	0.0051	0.006	0.026	0.007
Na caprate	1.8	-4.657	12.013	0.0213	0.2393	0.024	0.020	0.022
NaCl	6.144	-2.886	4.775	0.0097	0.0073	0.016	0.011	0.007
NaClO3	3	-0.665	0.001	0.0048	0.0039	0.004	0.005	0.005
NaClO4	6	-1.678	2.455	0.0070	0.0056	0.007	0.009	0.007
NaCNS	18	-3.150	4.795	0.0383	0.0231	0.065	0.039	0.037
NaF	1	-0.540	1.252	0.0009	0.0008	0.001	0.002	0.001
Na formate	3.5	-3.641	-9.313	0.0051	0.0045	0.005	0.008	0.005
NaH malonate	5	-1.072	2.902	0.0018	0.0015	0.001	0.001	0.002
NaH succinate	5	-1.951	4.153	0.0014	0.0014	0.002	0.002	0.001
NaH2PO4	6.5	-1.398	5.284	0.0042	0.0047	0.002	0.003	0.003
NaI	12	-4.043	6.547	0.0366	0.0204	0.091	0.028	0.034
NaNO3	10.83	-1.977	5.087	0.0729	0.0691	0.087	0.072	0.074
NaOH	29	-4.369	7.852	0.0880	0.0465	0.329	0.057	0.079
Na pelargonate	2.5	-3.802	10.329	0.0583	0.2331	0.062	0.058	0.059
Na propionate	3	-3.846	-7.309	0.0028	0.0024	0.003	0.008	0.003
NH4Cl	7.405	-1.307	2.140	0.0026	0.0025	0.001	0.002	0.002
NH4NO3	25.954	0.389	2.363	0.0155	0.1501	0.012	0.010	0.052
RbAc	3.5	-2.921	2.432	0.0057	0.0044	0.006	0.008	0.006
RbBr	5	-1.721	3.748	0.0041	0.0035	0.003	0.001	0.004
RbCl	7.8	-1.784	3.711	0.0057	0.0045	0.002	0.003	0.005
RbI	5	-1.871	4.069	0.0047	0.0042	0.003	0.002	0.004
RbNO3	4.5	-0.454	5.153	0.0096	0.0132	0.008	0.007	0.009
TiAc	6	-1.111	4.025	0.0122	0.0844	0.010	0.010	0.012
Overall				*0.0198*	*0.0238*	*0.041*	*0.017*	*0.018*
Uni-divalent								
Cs2SO4	1.8	-2.818	-7.921	0.0076	0.0079	0.009	0.008	0.008
K2SO4	0.7	-4.017	8.029	0.0076	0.0107	0.008	0.015	0.008
K2CrO4	3.5	-1.777	3.800	0.0150	0.0169	0.022	0.014	0.014
Li2SO4	3	-2.359	3.578	0.0162	0.0170	0.023	0.016	0.016

Table 1: The fitted parameters of the present model based on salt specific parameter approach and the relative standard deviation* of the present model and the E-NRTL-NRF and NWN [15] in correlating of the experimental activity coefficient and the prediction results of the present model in representing of experimental osmotic coefficient at 298 K. The uni-univalent experimental data were taken from [39] and the others from [40]. (Continued)

electrolyte	max. m	τ_{21}	τ_{12}	$\delta\gamma_\pm$	δ_Φ	$\delta\gamma_\pm$	$\delta\gamma_\pm$	$\delta\gamma_\pm$
Na2CrO4	4	-2.778	5.149	0.0402	0.0412	0.057	0.036	0.040
Na2SO4	4	-1.837	5.056	0.0119	0.0154	0.024	0.026	0.012
Na2S2O3	3.5	-2.308	4.782	0.0194	0.0213	0.03	0.017	0.020
(NH4)2SO4	4	-1.973	5.629	0.0244	0.0326	0.017	0.056	0.023
Rb2SO4	1.8	-1.744	-5.464	0.0069	0.0092	0.009	0.007	0.007
Overall				*0.0166*	*0.0191*	0.022	*0.022*	*0.016*
Di-univalent								
BaBr2	2	-4.820	-10.471	0.0229	0.0215	0.026	0.023	0.023
BaCl2	1.8	-5.169	-14.183	0.0188	0.0194			0.019
Ba(ClO4)2	5	-3.886	3.505	0.0424	0.0273	0.072	0.042	0.047
BaI2	2	-4.571	-5.703	0.0284	0.0255	0.034	0.029	0.033
Ba(NO3)2	0.4	-4.563	9.123	0.0031	0.0061			0.003
BaAc2	3.5	-5.177	-16.061	0.0128	0.0134			0.013
CaBr2	6	-6.404	10.220	0.1725	0.0705	0.351	0.279	0.135
CaCl2	6	-5.605	8.677	0.0825	0.0440	0.205		0.067
Ca(ClO4)2	6	-6.395	9.619	0.1071	0.0488	0.272	0.182	0.080
CaI2	2	-5.037	5.440	0.0331	0.0281	0.046	0.036	0.035
Ca(NO3)2	6	-2.645	2.899	0.0353	0.0272	0.06	0.034	0.036
Cd(NO3)2	2.5	-5.301	-14.352	0.0276	0.0251			0.027
CdCl2	6	-2.738	9.493	0.2630	0.7725	0.214	0.151	0.247
CdBr2	4	-4.325	11.557	0.3001	1.1244	0.258	0.197	0.275
CdI2	2.5	-6.359	15.041	0.4052	0.8642	0.374	0.301	0.361
CoBr2	5	-5.950	8.569	0.0484	0.0280	0.141	0.078	0.039
CoCl2	4	-4.635	5.782	0.0282	0.0214	0.055	0.027	0.028
CoI2	2	-6.689	9.928	0.0889	0.0403	0.242	0.172	0.085
Co(NO3)2	5	-4.836	6.777	0.0514	0.0323	0.108	0.042	0.043
CuCl2	6	-4.930	-12.530	0.0265	0.0206	0.038	0.036	0.027
Cu(NO3)2	6	-4.478	6.235	0.0482	0.0299	0.113	0.039	0.039
FeCl2	2	-3.913	-4.091	0.0239	0.0212	0.029	0.024	0.026
MgAc2	4	-3.130	4.716	0.0082	0.0082	0.013	0.010	0.007
MgBr2	5	-6.496	9.941	0.1099	0.0499	0.241	0.211	0.084
MgCl2	5	-6.037	9.324	0.0935	0.0482	0.202	0.179	0.076

Table 1: The fitted parameters of the present model based on salt specific parameter approach and the relative standard deviation* of the present model and the E-NRTL-NRF and NWN [15] in correlating of the experimental activity coefficient and the prediction results of the present model in representing of experimental osmotic coefficient at 298 K. The uni-univalent experimental data were taken from [39] and the others from [40]. (Continued)

electrolyte	max. m	τ_{21}	τ_{12}	$\delta\gamma_\pm$	δ_Φ	$\delta\gamma_\pm$	$\delta\gamma_\pm$	$\delta\gamma_\pm$
MgI2	5	-7.004	10.820	0.1509	0.0613	0.316	0.276	0.111
Mg(ClO4)2	4	-6.811	10.124	0.1089	0.0528	0.208	0.180	0.089
Mg(NO3)2	5	-5.093	7.161	0.0611	0.0359	0.125	0.048	0.052
MnCl2	6	-4.028	-5.732	0.0229	0.0183	0.047	0.024	0.024
NiCl2	5	-5.158	7.223	0.0348	0.0244	0.092	0.031	0.032
Pb(ClO4)2	6	-5.091	7.255	0.0592	0.0336	0.147	0.044	0.047
Pb(NO3)2	2	-2.896	7.756	0.0247	0.0454	0.022	0.017	0.024
SrBr2	2	-4.078	3.614	0.0300	0.0258	0.036	0.030	0.031
SrCl2	4	-4.844	6.973	0.0490	0.0339	0.088	0.044	0.047
Sr(ClO4)2	6	-5.724	8.231	0.0513	0.0265	0.168	0.080	0.040
SrI2	2	-4.664	4.383	0.0375	0.0296	0.046	0.038	0.040
Sr(NO3)2	4	-4.048	-11.519	0.0249	0.0274	0.029	0.027	0.025
UO2Cl2	3	-5.088	-9.870	0.0334	0.0239	0.04	0.034	0.034
UO2(ClO4)2	5.5	-7.784	12.137	0.1817	0.0659	0.447	0.443	0.103
UO2(NO3)2	5.5	-5.448	-11.245	0.0455	0.0293	0.041	0.042	0.043
ZnBr2	6	-5.527	-14.968	0.1188	0.0858			0.116
ZnCl2	6	-3.930	-9.602	0.1021	0.0917	0.119	0.107	0.106
ZnI2	6	-6.218	-17.566	0.1140	0.0738			0.107
Zn(ClO4)2	4	-6.943	10.504	0.1043	0.0500	0.211	0.210	0.081
Zn(NO3)2	6	-5.000	6.980	0.0653	0.0357	0.148	0.051	0.051
Overall				*0.0778*	*0.0953*	0.139	*0.100*	*0.068*
Di-divalent								
BeSO4	4	-5.834	10.074	0.0590	0.1193	0.039	0.078	0.055
MgSO4	3.5	-5.695	10.071	0.0563	0.1335	0.036	0.074	0.054
MnSO4	4	-5.353	9.759	0.0529	0.1265	0.037	0.084	0.050
NiSO4	2.5	-5.792	10.584	0.0506	0.1332	0.031	0.072	0.048
CuSO4	1.4	-6.588	11.917	0.0532	0.1412	0.037	0.067	0.052
ZnSO4	3.5	-5.719	10.407	0.0526	0.1316	0.038	0.083	0.050
CdSO4	3.5	-5.308	9.853	0.0567	0.1325	0.037	0.073	0.053
UO2SO4	6	-4.834	8.777	0.0857	0.1224	0.05	0.054	0.075
Overall				*0.0584*	*0.130*	0.038	*0.073*	*0.054*

Table 1: The fitted parameters of the present model based on salt specific parameter approach and the relative standard deviation* of the present model and the E-NRTL-NRF and NWN [15] in correlating of the experimental activity coefficient and the prediction results of the present model in representing of experimental osmotic coefficient at 298 K. The uni-univalent experimental data were taken from [39] and the others from [40]. (Continued)

electrolyte	max. m	τ_{21}	τ_{12}	$\delta\gamma_\pm$	$\delta\Phi$	$\delta\gamma_\pm$	$\delta\gamma_\pm$	$\delta\gamma_\pm$
Tri-univalent								
AlCl3	1.8	-6.175	7.915	0.0822	0.0610	0.115	0.080	0.080
CeCl3	2	-4.718	4.074	0.0638	0.0521	0.084	0.063	0.065
CrCl3	1.2	-6.480	-17.152	0.0498	0.0460	0.069	0.073	0.049
Cr(NO3)3	1.4	-6.162	-15.242	0.0492	0.0445	0.054	0.070	0.049
EuCl3	2	-4.963	4.761	0.0694	0.0561	0.091	0.068	0.071
LaCl3	2	-4.565	-3.720	0.0644	0.0542	0.082	0.063	0.065
NdCl3	2	-4.896	4.860	0.0621	0.0516	0.083	0.061	0.064
PrCl3	2	-4.740	4.250	0.0627	0.0533	0.082	0.062	0.064
ScCl3	1.8	-5.208	5.019	0.0590	0.0482	0.078	0.059	0.060
SmCl3	2	-4.916	4.695	0.0653	0.0536	0.087	0.064	0.067
YCl3	2	-4.534	-0.012	0.0744	0.0578	0.093	0.064	0.066
Overall				*0.0638*	*0.0526*	*0.083*	*0.066*	*0.064*

$$*\; \delta = \sqrt{\frac{1}{Np}\sum_i^{NP}\left(\ln\left.\gamma_1^{exp}\right|_i - \ln\left.\gamma_1^{cal}\right|_i\right)^2}$$ *where γ_1^{exp} , γ_1^{cal} and NP are experimental and calculated mean activity coefficient and number of the data points, respectively.*
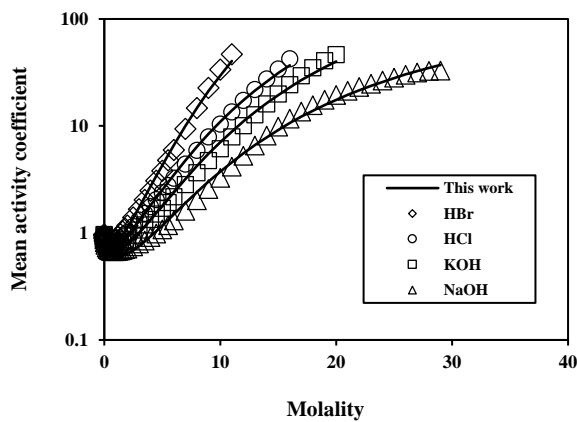
Fig. 1: The comparison of the results of the new model with the experimental data [40] in correlating activity coefficients of various uni-univalent electrolytes at 298 K.
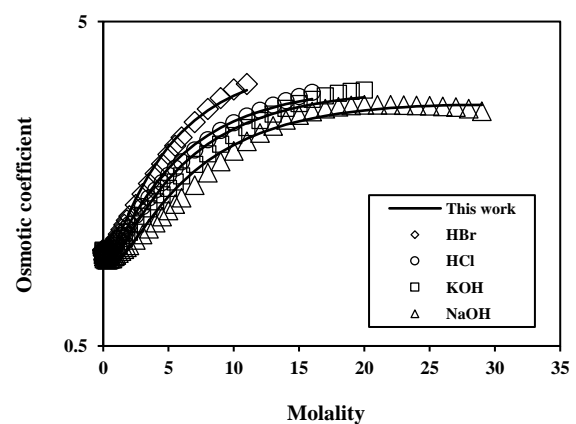
Fig. 2: Prediction of the osmotic coefficients [40] of some uni-divalent electrolytes at 298 K.

electrolytes up to saturation molalities. As one can see the results of the prediction are satisfactory.

Strong aqueous ternary electrolyte

The extension of the present model for strong aqueous ternary electrolyte systems has been also done. The results of the new model in predicting experimental osmotic

coefficients of a number of ternary aqueous electrolytes have been given in Table 3. The overall relative standard deviation is 0.046 indicating good predictability of the present model.

The solubility diagrams for various salt/salt/water systems were also predicted by the new model. The phase diagram construction (solid-liquid equilibrium) is done using the following equation.

Table 2: The relative standard deviation* of the present model in predicting experimental osmotic coefficient of some aqueous ternary electrolytes at 298 K.

Salt 1	Salt 2	δΦ	Data Ref.
		Salt specific	
NaCl	KCl	0.015	[47]
(NH4Cl)	(NaCl)	0.013	[48]
LiCl	MgCl2	0.075	[49]
(NH4)2SO4	K2SO4	0.021	[50]
NaCl	LiCl	0.034	[51]
LiCl	CsCl	0.053	[52]
NH4NO3	LiNO3	0.087	[53]
MgCl2	Mg(NO3)2	0.069	[54]
Ave.		0.046	
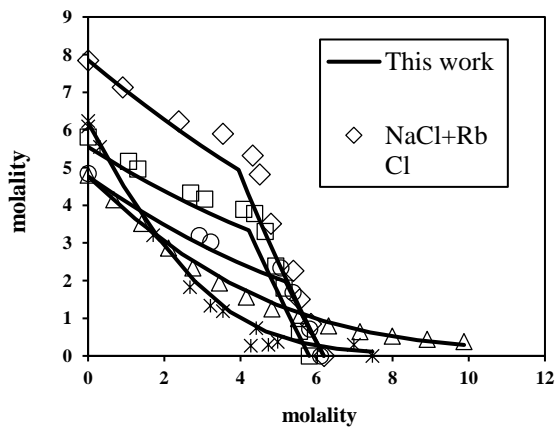
Fig. 3: Solubility [59] diagram prediction for aqueous NaCl-RbCl, NaCl-KCl, KBr-CsBr, KCl-HCl and NaCl-CaCl₂ at 298 K.

$$K_{sp} = \left(m_c \gamma_c^{m,*} \right)^{\upsilon_c} \left(m_a \gamma_a^{m,*} \right)^{\upsilon_a} = \tag{20}$$

$$\left(m_c \right)^{\upsilon_c} \left(m_a \right)^{\upsilon_a} \left(\gamma_\pm^{m,*} \right)^{\upsilon_a + \upsilon_c}$$

Where K_{sp}, m_c, and m_a are solubility product, cation, and anion molalities, respectively. In the salt specific parameter approach, for a ternary system such as NaCl (1)+KCl (2)+water (3), one should first expand Eq. (11) with n=3. The mean activity coefficient of the NaCl or KCl can be calculated after unsymmetrical normalization ($\gamma_{NaCl,\pm}^* = \gamma_2^*$ and $\gamma_{KCl,\pm}^* = \gamma_3^*$). The results have been shown in Fig. 3 for aqueous solutions of NaCl+KCl, HCl+KCl, NaCl+RbCl, KBr+CsBr, NaCl+CaCl₂ [59, 60]. As one can see the prediction results are good.

CO₂+NaCl+H₂O system

The capability of the modified model has been more checked by considering the ternary system of CO₂+NaCl+H₂O. The sub-binary systems of this ternary system are NaCl+H₂O and CO₂+H₂O. The results and the parameters of the modified model for the NaCl+H₂O system have been presented in the previous sections. As mentioned, the present model reduces to the NRTL model [36] in the absence of ions in the solution, so the interaction parameters of the NRTL model can be used for this binary. The VLE calculation based on the gamma-phi approach is done by the following equations. For solvent

$$y_w \varphi_w P = x_w p_w^{sat} \varphi_w^{sat} \gamma_w \exp \left(\frac{\nu_w \left(P - p_w^{sat} \right)}{RT} \right) \tag{21}$$

For CO₂,

$$y_{CO_2} \varphi_{CO_2} P = x_{CO_2} H_{CO_2} \gamma_{CO_2}^* \exp \left(\frac{\nu_{CO_2}^\infty \left(P - p_w^{sat} \right)}{RT} \right) \tag{22}$$

Where y and x stand for vapor and liquid phase mole fractions. φ denotes fugacity coefficient of the gas phase. P is total pressure. p_w^{sat} is the vapor pressure of water at system temperature, T. H is the Henry's constant of CO₂ in water at T and at water saturation vapor pressure. ν_w is the water molar volume at T and $\nu_{CO_2}^\infty$ is the partial molar volume of CO₂ at infinite dilution in water. In this work, $\nu_{CO_2}^\infty$
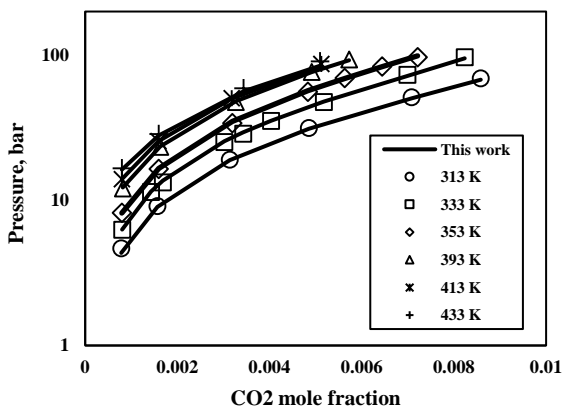
Fig. 4: The correlation results of the present model for ternary CO2+NaCl+H2O system, experimental data from [63].

is calculated using the Brelvi-O'Connell model [61]. The SRK EOS has been used for fugacity coefficient of the vapor phase.

In this work, the interaction parameters of NRTL model [36] for CO_2+H_2O binary system were taken from the work of Chen and Evans [12] that are $\tau_{water-CO2} = \tau_{CO2-water} = 10.0640 -3268.135/T$.
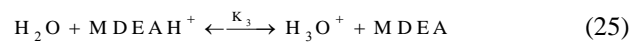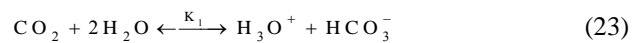
The experimental data of *Rumpf et al.* [62] at the temperature range of 313-433 K and pressure range of 4.7-96.4 bar (63 data points) have been used to study the ternary system of $CO_2+NaCl+H_2O$ ternary system. Using the fitted parameters of $NaCl+H_2O$ and CO_2+H_2O, the remaining adjustable parameters are $\tau_{NaCl-CO2}$ and $\tau_{CO2-NaCl}$ for a salt-specific approach. These parameters have been obtained using the experimental data of *Rumpf et al.* [62] that are $\tau_{NaCl-CO2} =126.074-11918.73/T$ and $\tau_{CO2-NaCl} = -120.057 + 8043.950/T$. The AAD% of the model is 1.7% indicating very good results of the present model. Fig. 7 shows the results of the correlation. As one can see the agreements are very good.

Weak electrolyte with multi solvents (H2S or CO2+Water+ MDEA)

In this section the performance of the new model is shown in a weak electrolyte, as well as the solubility of two weak acid gases, H_2S and CO_2, in aqueous Methyldiethanolamine (MDEA) solution at various conditions is calculated. Modeling of acid gas solubility in aqueous alkanolamines solutions is important from both theoretical viewpoint and industrial applications, especially in natural gas sweetening and flue gas treatment.

In a general categorization, studying the thermodynamics of such systems is accomplished by using two types of models: an activity coefficient equation [63–68] or an electrolyte equation of state [10, 69, 70]. In this section, the modified N-NRTL-NRF activity coefficient model is extended to correlate solubility of CO_2 and H_2S in aqueous MDEA solution at various temperatures, concentrations, and pressures.

In the liquid phase of these systems a number of ionic species are produced according to the following equilibrium reactions:

$$CO_2 + 2H_2O \xleftrightarrow{K_1} H_3O^+ + HCO_3^- \qquad (23)$$

$$H_2S + H_2O \xleftrightarrow{K_2} H_3O^+ + HS^- \qquad (24)$$

$$H_2O + MDEAH^+ \xleftrightarrow{K_3} H_3O^+ + MDEA \qquad (25)$$

The thermodynamic equilibrium constant for the above reactions is expressed as follows:

$$K = \prod_i a_i^{v_i} = \prod_i (x_i \gamma_i)^{v_i} \qquad (26)$$

Where a_i, x_i, γ_i and v_i are the activity, mole fraction, activity coefficient, and reaction stoichiometry of the species i respectively. Activity coefficients of all species are calculated using the present model in this work.

Due to the low concentration of acid gases in the liquid phase, one is allowed to assume that the partial pressure of the molecular species CO_2 and H_2S is expressed as follows:

$$P_i = x_i H_i \qquad (i = CO_2, H_2S) \qquad (27)$$

Where H_i and P_i are Henry's constant and partial pressure of species i (CO_2 and H_2S) respectively.

The thermodynamic equilibrium constant used this work is based on the mole fraction scale and Henry's constant has the unit of Pascal. The temperature dependence of the equilibrium constants and Henry's constants are expressed as:

$$\ln K_i (or H) = C_1 + C_2 / T + C_3 \ln T + C_4 T \qquad (28)$$

The coefficients C_1-C_4 for all reactions and Henry's constants that were used in this work are listed in Table 3.

For simplification, due to the low concentration of molecular species of CO_2 and H_2S and the ionic species of CO_3^{2-} and S^{2-} in the aqueous phase in comparison with

Table 3: Temperature Dependence of the equilibrium Constant of reactions and Henry's constant of CO_2 and H_2S.

Reaction	Compound	C1	C2	C3	C4	Reference
1	CO_2	231.465	-12092.1	-36.7816	0.0	[63]
2	H_2S	214.582	-12995.4	-33.5471	0.0	[63]
3	MDEA	-56.27	-4044.8	7.848	0.0	[64]
Henry's constant	CO2	110.03	-6789.04	-11.452	-0.0105	[64]
Henry's constant	H2S	358.138	-13236.8	-55.0551	0.059565	[63]

the other species in the system, we neglect the concentration of these species. Therefore, for the CO_2-MDEA-H_2O and H_2S-MDEA-H_2O systems, there are four species in the liquid phase. Two species are MDEA and water that are natural solvents and two species are protonated amine and bicarbonate ion or bisulfide ion, (bicarbonate ion form in systems that contain CO_2 and bisulfide ion form in systems that contain H_2S), which are ionic species.

Calculations for the above two systems are similar. For example, in the CO_2-MDEA–H_2O system, the mass balance equations can be written as:

$$C_{MDEAH^+} = C_{HCO_3^-} = C_{MDEA}^0 \alpha \qquad (29)$$

$$C_{MDEA}^0 = C_{MDEA} = C_{MDEAH^+} \qquad (30)$$

$$C_{H_2O}^0 = C_{H_2O} + C_{MDEAH^+} \qquad (31)$$

Where (^{0}) represents the initial concentration of species and α denotes the acid gas loading in the liquid phase.

From the reactions (23) and (25) we can obtain as:

$$CO_2 + H_2O + MDEA \xleftrightarrow{K_1/K_3} MDEAH^+ + HCO_3^- \quad (32)$$
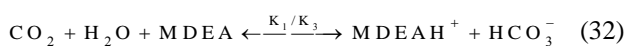
So using Eq. (26), one can write the equation of the equilibrium constants for Reactions (32) and (25) and combine with Eq. (27), the partial vapor pressure of CO_2 is obtained as:

$$P_{CO_2} = \frac{H_{CO_2} K_3 x_{MDEAH^+} \gamma^*_{MDEAH^+} x_{CHCO_3^-} \gamma^*_{CHCO_3^-}}{k_1 x_{H_2O} \gamma_{H_2O} x_{MDEA} \gamma_{MDEA}} \qquad (33)$$

Thus, using the equilibrium solubility experimental data of CO_2 in an aqueous MDEA solution, the energy interaction parameters for the CO_2-MDEA-H_2O system are obtained using the objection function as [65, 66]

$$OF = \frac{1}{N} \sum_N \left| \frac{\left(P_{CO_2}\right)_{cal} - \left(P_{CO_2}\right)_{exp}}{\left(P_{CO_2}\right)_{exp}} \right| \qquad (34)$$

However, the interaction energy parameters of the H_2S-MDEA-H_2O system are obtained by using the experimental solubility data through a different objection function as [65, 66]

$$OF = \frac{1}{N} \sum_N \left[\frac{\left(\left(P_{H_2S}\right)_{cal} - \left(P_{H_2S}\right)_{exp}\right)^2}{\left(P_{H_2S}\right)_{cal} - \left(P_{H_2S}\right)_{exp}} \right] \qquad (34)$$

Where N in Eqs. (34) and (35) represent the number of data points for each system.

Because the experimental data are in the wide range of temperatures and we correlate experimental data globally, it is assumed that interaction energy parameters have a dependency of temperature as the following function:

$$\tau_{ij} = a_{ij} \frac{b_{ij}}{T} \qquad (36)$$

Where a_{ij} and b_{ij} are the coefficients of the interaction energy parameters and T is temperature. To obtain a reliable set of interaction energy parameters, a large number of experimental data from open literature [71-77], 213 data points for the CO_2-MDEA-H_2O system, and 152 data points for the H_2S-MDEA-H_2O system, have been used. The coefficients of interaction energy parameters for these two systems are presented in Table 4. The percent of average absolute deviation (δ %) of the present model (modified N-NRTL-NRF) is given in Tables 5 and 6 for CO_2-MDEA-H_2O and H_2S-MDEA-H_2O systems, respectively, and compared with two other models namely N-NRTL-NRF [22] and Clegg–Pitzer [66] equations. Since the same data are used in these three models for both

Table 4: Values of coefficients of the interaction parameters for ternary systems CO₂-MDEA-H₂O and H₂S-MDEA-H₂O[a].

Parameter	Coefficient	
τ_{ij}	a_{ij}	b_{ij}
	H_2O-MDEA-CO_2	
$\tau_{1,2}$	12.138	-
$\tau_{2,1}$	9.1303	-
$\tau_{1,MX}$	4.5540	1497.7
$\tau_{MX,1}$	-6.6254	4812.1
$\tau_{2,MX}$	-1.5259	-749.48
$\tau_{MX,2}$	-7.4763	6746.6
	H_2O-MDEA-H_2S	
$\tau_{1,MY}$	5.8614	1007.8
$\tau_{MY,1}$	-30.823	13813
$\tau_{2,MY}$	-2.6113	-494.16
$\tau_{MY,2}$	93.499	-22870

[a] $1 = H2O; 2 = MDEA; M = MDEAH^+; X = HCO_3^- ; Y = HS^-.$

ternary systems, a fair comparison can be made. It should be noted that the results of the modified N-NRTL- NRF model similar to the N-NRTL-NRF model and the Clegg–Pitzer equation present a good agreement with the experiment. Thus, one can see that the present model can be applied successfully for the calculation of the (vapor + liquid) equilibrium of the acid gas aqueous MDEA systems.

As shown in Tables 5 and 6, the modified version of the N-NRTL-NRF model shows better results with respect to the original version of this model for the CO_2-MDEA-H_2O system, however, for the H_2S-MDEA-H_2O system two models demonstrate similar behavior. For the CO_2-MDEA-H_2O system, the present model shows the deviation equal to 30.3% (δ=30.3%) so that the deviation of the original version of the model with experimental data is δ=34.3%. Therefore, in general, it can be concluded that the new model with respect to the original model displays better accuracy. Also, the comparison between the modified N-NRTL-NRF with the Clegg–Pitzer model shows that for the CO_2-MDEA-H_2O system, the Clegg–Pitzer model with δ= 25.7 % demonstrates better accuracy than the modified N-NRTL-NRF model with δ= 30.3 %, however, for the H_2S-MDEA-H_2O system the modified N-NRTL-NRF

model with δ= 24.8 % shows better precision than Clegg–Pitzer model with δ= 30.6 %. So, the ability of these two models for correlation of the solubility of the acid gases in the aqueous MDEA solutions is similar.

Figs. 5 and 6 present the partial pressure of CO_2 versus acid gas loading at different temperatures and concentrations of MDEA. Also, Figs. 7 and 8 show the results of the partial pressure of H_2S against acid gas loading at various temperatures and concentrations of MDEA. Finally, Fig. 9 presents the deviation analysis of the partial pressure as $\left(P_{cal} - P_{exp} \right) / P_{exp}$, versus acid gas loading for both the CO_2-MDEA-H_2O and H_2S-MDEA-H_2O systems. As one can see at high acid gases loading more deviation can be observed for both ternary systems and the model more shows the higher correlation $\left(\left(\left(P_{cal} - P_{exp} \right) / P_{exp} \right) > 1 \right)$.

CONCLUSIONS

A new electrolyte model composed of a nonelectrolyte equation that is derived based on local composition concept as the short-range contribution and the Pitzer-Debye-Hückel equation as the long-range contribution was successfully developed. The modification has been done

Table 5: The averagedeviation of partial pressure data for the CO₂-MDEA-H₂O system.

MDEA Concentration/wt% [data ref.]	Temperature /°C	Clegg –Pitzer [66]	N-NRTL-NRF [22]	This work
		No. of data points, δ (%)[a]	No. of data points, δ (%)[a]	No. of data points, δ(%)[a]
11.8 [71]	25	4, 15.7	4, 57.9	4, 40.8
20.0 [71]	37.8, 65.6, 115.6	31, 8.96	30, 49.5	30, 40.2
23.3 [71]	25, 50	15, 32.9	15, 60.7	15, 57.0
23.3 [72]	25, 40, 70, 100, 120	34, 40.3	35, 33.0	35, 36.9
23.3 [73]	40	4, 15.9	4, 46.0	4, 35.7
23.3 [74]	40	8, 15.2	8, 16.9	8, 12.0
30.0 [75]	25, 40, 80, 120	24, 20.1	25, 32.9	25, 27.8
35.0 [76]	40, 100	37, 19.4	37, 22.4	37, 21.7
48.8 [72]	25, 40, 70, 100, 120	48, 20.1	48, 28.9	48, 22.9
49.0 [77]	40, 100	7, 23.7	7, 24.8	7, 15.8
Total		**213, 25.7**	**213, 34.3**	**213, 30.3**

[a] $\delta(\%) = 100\ (1/N)\sum_1^N \left| \left[(P_{CO_2})_{cal} - (P_{CO_2})_{exp} \right]/(P_{CO_2})_{exp} \right|$

Table 6: The average deviation of partial pressure data for the H2S-MDEA-H2O system.

MDEA concentration/ wt% [data ref.]	Temperature /°C	Clegg –Pitzer [66]	N-NRTL-NRF[22]	This work
		No. of data points, δ (%)[a]	No. of data points, δ (%)[a]	No. of data points,, δ(%)[a]
11.8 [71]	25	7, 30.2	7, 40.6	7, 38.7
20.0 [71]	37.8, 65.6, 115.6	20, 17.9	18, 32.2	18, 22.3
23.3 [72]	40, 100	17, 51.0	17, 30.0	17, 27.5
23.3 [73]	40	21, 43.5	23, 33.7	23, 39.9
35.0 [76]	40, 100	35, 21.0	35, 17.1	35, 16.3
48.8 [76]	40	14, 41.6	14, 26.0	14, 27.6
48.8 [72]	25, 40, 70, 100, 120	40, 26.5	38, 17.4	38, 23.3
Total		**154, 30.6**	**152, 24.8**	**152, 24.8**

[a] $\delta(\%) = 100\ (1/N)\sum_1^N \left| \left[(P_{H_2S})_{cal} - (P_{H_2S})_{exp} \right]/(P_{H_2S})_{exp} \right|$

in the adoption of reference states for electrolyte and water, so the modified new model can be reduced to the nonelectrolyte NRTL model in the absence of electrolyte. The new model has two parameters per each salt in the first step, the modified model is applied for the representation of activity coefficients and osmotic coefficient of various aqueous strong electrolyte solutions at a wide range of molalities at 298 K. The comparisons of the new model with E-NRTL, E-NRTL-NRF and nonelectrolyte Wilson-

NRF models confirm the good capability of the new model. In addition, the predictions of osmotic coefficients and solubilities of several aqueous ternary systems have been successfully carried out by the new model. Furthermore, the correlation of CO_2 solubility in aqueous NaCl has been carried out with good accuracy. The computations of acid gas solubilities in aqueous MDEA solutions were well done. The comparisons of the results with the Clegg–Pitzer and the nonelectrolyte NRTL-NRF
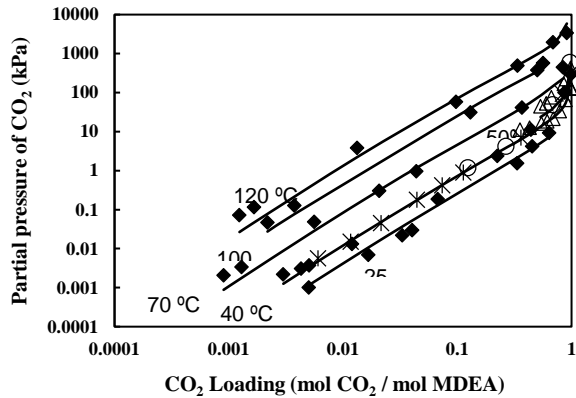
Fig. 5: The solubility of CO_2 in 23.3 wt% MDEA aqueous solution at 25, 40, 50, 70, 100, and 120 °C. Symbols represent experimental data: (△), Maddox et al. [71]; (♦), Jou et al. [72]; (○), MacGregor and Mather [74]; (*), Austgen and Rochelle[68]; (—) this work (modified N-NRTL-NRF model).
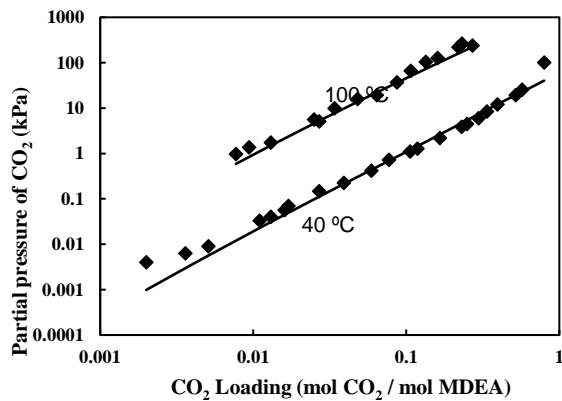

Fig. 6: The solubility of CO_2 in 35 wt% MDEA aqueous solution at 40 and 100 °C. Symbols represent experimental data: (♦), Jou et al. [76]; (—) this work (modified N-NRTL-NRF model).
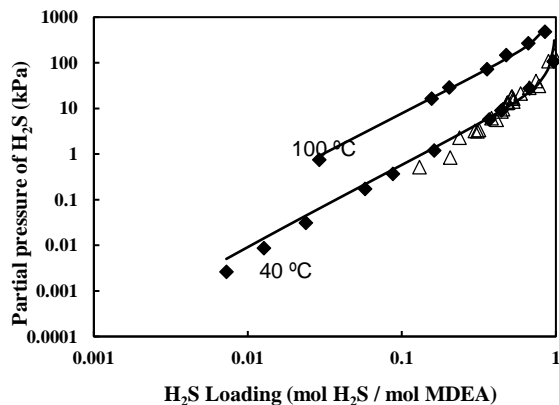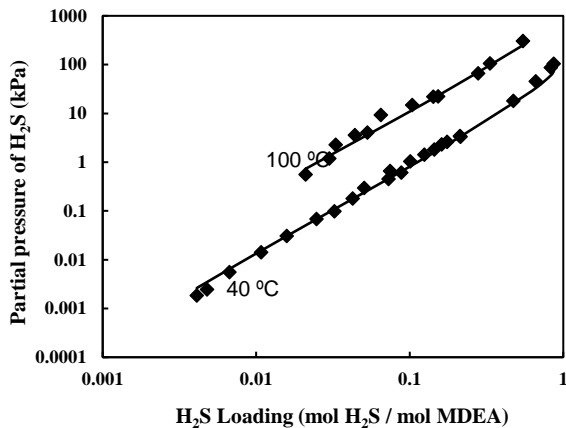

Fig. 7: The solubility of H_2S in 23.3 wt% MDEA aqueous solutions at 40 and 100°C. Symbols represent experimental data: (♦), Jou et al. [72]; (△), MacGregor and Mather [73]; (—) this work (modified N-NRTL-NRF model).

model proves again the good capability of the modified model for weak electrolyte systems. The results given in all tables and figures indicate that the modified model is capable to successfully correlate and predict the experimental data of aqueous strong electrolyte solutions at wide ranges of molalities, temperatures, and pressures. Simplicity, good accuracy, and reduction to the NRTL equation in the absence of ions are the main advantages of the present model.

Nomenclature

A_φ	Pitzer- Debye–Hückel constant
g	Gibbs energy function, J/mol
I_x	Ionic strength in mole fraction based
m	Molality, mol/kg
M_w	Molecular weight of water/ kg/kmol
NP	Number of experimental points
R	Universal gas constant
T	Absolute temperature
x,y	Mole fraction
z	Charge number of ionic species

Greek symbols

α	Non-randomness factor
γ	Activity coefficient
v	Stoichiometric number
Γ	Nonrandom factor
ρ	Closest ion approach parameter
τ	Interaction energy parameter
Φ	Osmotic coefficient
φ	Fugacity coefficient

Superscripts

cal	Calculated
exp	Experimental
E	Excess
LR	Long-range
SR	Short-range
Ref	Reference state
W	Water
*	Unsymmetrical convention
∞	Infinite dilution

Subscripts

a	Anion
c	Cation

Fig. 8: The solubility of H₂S in 35wt% MDEA aqueous solutions at 40 and 100°C. Symbols represent experimental data:(♦), Jou et al. [76]; (—) this work (modified N-NRTL-NRF model).
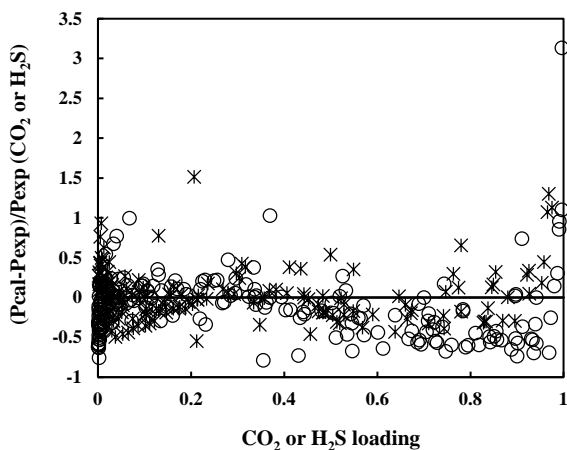

Fig. 9: Comparison of the correlated with the experimental data for CO₂ and H₂S equilibrium partial pressure in aqueous MDEA solution at various temperature and concentration. (○), CO₂-MDEA-H₂O system [71-77]; (*), H₂S-MDEA-H₂O system [71–73,76].

| w | Water |
| ± | Mean |

REFERENCES

[1] Prausnitz J. M., Lichtenthaler R. N., de Azevedo E. G., "Molecular Thermodynamics of Fluid-phase Equilibria", 3rd ed., Prentice Hall PTR, New Jersey, (1999).

[2] Zemaitis J.F., Clark D.M., Rafal M., Scrivner N.C., "Handbook of Aqueous Electrolyte Thermodynamics", American Institute of Chemical Engineers, N.Y, (1986).

[3] Fürst W., Renon H., Representation of Excess Properties of Electrolyte Solutions Using a New Equation of State, *AIChE J.,* **39**: 335–343 (1993).

[4] Myers Jason A., Sandler S. I., Wood R. H., An Equation of State For Electrolyte Solutions Covering Wide Ranges of Temperature, Pressure, and Composition, *Ind. Eng. Chem. Res.,* **41**: 3282–3297 (2002).

[5] Lin Y., Thomsen K., de Hemptinne J.C., Multicomponent Equations of State for Electrolytes, *AIChE J.,* **53**: 989–1005 (2007).

[6] Wu J., Pausnitz J. M, Phase Equilibria for Systems Containing Hydrocarbons, Water, and Salt: an Extended Peng-Robinson Equation of State, *Ind. Eng. Chem. Res.*, **37**: 1634–1643 (1998).

[7] Haghtalab A., Mazloumi S.H., A new coordination Number Model for Development of a Square-Well Equation of State, *Fluid Phase Equilib.,* **280**: 1–8 (2009).

[8] Haghtalab A., Mazloumi S.H., A Square-Well Equation of State for Aqueous Strong Electrolyte Solutions, *Fluid Phase Equilib.,* **285**: 96–104 (2009).

[9] Mazloumi S.H., Correlation of the Mean Activity Coefficient of Aqueous Electrolyte Solutions Using an Equation of State, *Chin. J. Chem. Eng.,* **24**: 1456–1463 (2016).

[10] Haghtalab A., Mazloumi S.H., Electrolyte Cubic Square-Well Equation of State for Computation of the Solubility CO₂ and H₂S in Aqueous MDEA Solutions, *Ind. Eng. Chem. Res.,* **49**: 6221-6230 (2010).

[11] Cruz J., H. Renon H., A New Thermodynamic Representation of Binary Electrolyte Solutions Nonideality in the Whole Range of Concentrations, *AIChE J.,* **24**: 817-829 (1978).

[12] Chen C.-C., Evans L.B., Local Composition Model for the Excess Gibbs Energy of Aqueous Electrolyte Systems, *AIChE J.,* **32**:444-454 (1986).

[13] Zhao E., Yu M., Sauve R.E., Khoshkbarchi M.K., Extension of the Wilson Model to Electrolyte Solutions, *Fluid Phase Equilib.*, **173**: 161-175 (2000).

[14] Haghtalab A., Vera J.H., A nonrandom Factor Model for the Excess Gibbs Energy of Electrolyte Solutions, *AIChE J.,* **34**: 803–813 (1988).

[15] Sadeghi R., New Local Composition Model for Electrolyte Solutions, *Fluid Phase Equilib.,* **231**: 53–60 (2005).

[16] Liu Y., Harvey A.H., Prausnitz J.M., Thermodynamics of Concentrated Electrolyte Solutions, *Chem. Eng. Commun*., **77**: 43-66 (1989).

[17] Jaretun A., Aly G., New local Composition Model for Electrolyte Solutions: Single Solvent, Single Electrolyte Systems, *Fluid Phase Equilib.,* **163**: 175-193 (1999).

[18] Xu X., Macedo E. A., New Modified Wilson Model for Electrolyte Solutions, *Ind. Eng. Chem. Res.,* **42**: 5702–5707 (2003).

[19] Haghtalab A., Peyvandi K., Generalized Electrolyte-UNIQUAC-NRF Model for Calculation of Solubility and Vapor Pressure of Multicomponent Electrolytes Solutions, *Fluid Phase Equilib.,* **281**: 163–171 (2009).

[20] Pazuki G.R., Rohani A.A., Dashtizadeh A., Correlation of the Mean Ionic Activity Coefficients of Electrolytes in Aqueous Amino Acid and Peptide Systems, *Fluid Phase Equilib.,* **231**: 171-175 (2005).

[21] Haghtalab A., Mazloumi S.H., A Nonelectrolyte Local Composition Model and Its Application in the Correlation of The Mean Activity Coefficient of Aqueous Electrolyte Solutions, *Fluid Phase Equilib.,* **275**: 70-77 (2009).

[22] Haghtalab A., Shojaeian A., Mazloumi S.H., Nonelectrolyte NRTL-NRF Model to Study Thermodynamics of Strong and Weak Electrolyte Solutions, *J. Chem. Thermodyn.,* **43**: 354-363 (2011).

[23] Lu X., Zhang L., Wang Y., Shi J., Maurer G., Prediction of Activity Coefficients of Electrolytes in Aqueous Solutions at High Temperatures, *Ind. Eng. Chem. Res.,* **35**: 1777-1784 (1996).

[24] Christensen C., Sander B., Fredenslund A., Rasmussen P., Towards the Extension of UNIFAC to Mixtures with Electrolytes, *Fluid Phase Equilib.,* **13**:297-309 (1983).

[25] Thomsen K. Modeling Electrolyte Solutions with the Extended Universal Quasichemical (UNIQUAC) Model, *Pure Appl. Chem.,* **77**: 531–542 (2005).

[26] Song Y., Chen C.-C., Symmetric Nonrandom Two-Liquid Segment Activity Coefficient Model for Electrolytes, *Ind. Eng. Chem Res.,* **48**: 7788-7797 (2009).

[27] Mazloumi S. H., Representation of Activity and Osmotic Coefficients of Electrolyte Solutions Using Non-Electrolyte Wilson-NRF Model with Ion-Specific Parameters, *Fluid Phase Equilib.*, **388**: 31–36 (2015).

[28] Mazloumi S. H., An Ion-Based Nonelectrolyte NRTL-NRF for Aqueous Electrolyte Solutions, *CALPHAD*, **51**: 299–305 (2015).

[29] Mazloumi S. H., On the Application of Nonelectrolyte UNIQUAC-NRF Model for Strong Aqueous Electrolyte Solutions, *Fluid Phase Equilib.,* **417**: 70–76 (2016).

[30] Zafarani-Moattar M.T., Majdan-Cegincara, R., New Local Composition Model For Modeling of Thermodynamic and Transport Properties of Binary Aqueous Electrolyte Solutions, *CALPHAD*, **35**: 109-132 (2011).

[31] Zafarani-Moattar M.T., Majdan-Cegincara, R., Applicability of Different Equations In Modeling the Thermodynamic and Transport Properties of Aqueous and Non-Aqueous Ionic Liquid Solutions, *Fluid Phase Equilib.,* **386**:82-95 (2015).

[32] Mohammadian Abriz A., Majdan Cegincara R., Modeling the Transport and Volumetric Properties of Solutions Containing Polymer and Electrolyte with New Model, *Iran. J. Chem. Chem. Eng. (IJCCE),* **37(4)**: 235-252 (2018).

[33] Mazloumi S.H., Shojaeian A., Modified Nonelectrolyte Wilson-NRF: A New Model for Strong and Weak Electrolyte Solutions, *J. Mol. Liquids,* **277**:714-725 (2019).

[34] Haghtalab A., Joda M., Modification of NRTL-NRF Model For Computation of Liquid-Liquid Equilibria in Aqueous Two-Phase Polymer–Salt Systems, *Fluid Phase Equilib.,* **278**: 20-26 (2009).

[35] Pahlevanzadeh H., Mohseni-Ahooei A., Estimation of UNIQUAC-NRF Model Parameters for NH_3-CO_2-H_2O System, *Iran. J. Chem. Chem. Eng. (IJCCE),* **24(1)**: 21-26 (2005).

[36] Renon H., Prausnitz J. M., Local Composition in Thermodynamic Excess Functions for Liquid Mixtures, *AIChE J.,* **14**: 135-144 (1986).

[37] Wilson G. H. Vapor-Liquid Equilibrium. XI. A New Expression for Excess Free Energy of Mixing, *J. Am. Chem. Soc.*, **86**:127-130 (1964).

[38] Abrams D.S., Prausnitz J.M., Statistical Thermodynamics of Liquid Mixtures: A New Expression for The Excess Gibbs Energy of Partly or Completely Miscible Systems, *AIChE J.,* **21**: 116-128 (1975).

[39] Robinson R.A., Stokes R.H., "Electrolyte Solutions", 2nd ed., Butterworthm, London, (1965).

[40] Hamer W. J., Wu Y. C., Osmotic Coefficients and Mean Activity Coefficients of Uni-Univalent Electrolytes In Water At 25° C, *J. Phys. Chem. Ref. Data,* **1**: 1074-1099 (1972).

[41] Holmes H., Mesmer R. Thermodynamics of Aqueous Solutions of the Alkali Metal Sulfates, *J. Solution Chem.,* **15**: 495-517 (1986).

[42] Archer D. G., Thermodynamic Properties of the KCl+ H_2O System, *J. Phys. Chem. Ref. Data*, **28**: 1-16 (1999).

[43] Archer D.G., Thermodynamic Properties of the $NaNO_3$+ H_2O System, *J. Phys. Chem. Ref. Data*, **29**: 1141-1156 (2000).

[44] Pitzer K. S., Peiper J. C., Busey R. Thermodynamic properties of Aqueous Sodium Chloride Solutions, *J. Phys. Chem. Ref. Data,* **13**: 1-102 (1984).

[45] Archer D.G., Thermodynamic properties of the NaBr+ H_2O System, J. *Phys. Chem. Ref. Data,* **20**: 509-555 (1991).

[46] Ananthaswamy J., Atkinson G., Thermodynamics of Concentrated Electrolyte Mixtures. 5. A Review of the Thermodynamic Properties of Aqueous Calcium Chloride in the Temperature Range 273.15-373.15 K, *J. Chem Eng. Data,* **30**: 120-128 (1985).

[47] Dinane A., El Guendouzi M., Mounir A., Hygrometric Determination of Water Activities, Osmotic and Activity Coefficients of (NaCl+ KCl) (aq) at T= 298.15 K, *J. Chem. Thermodyn.*, **34**: 423–441 (2002).

[48] Dinane A., El Guendouzi M., Mounir A., Hygrometric Determination of the Water Activities and the Osmotic and Activity Coefficients of (ammonium chloride+ sodium chloride+ water) at T= 298.15 K, *J. Chem. Thermodyn.,* **34**: 783-793 (2002).

[49] Azougen R., El Guendouzi M., Rifai A., Faridi, J., Water Activities, Activity Coefficients and Solubility in the Binary and Ternary Aqueous Solutions with Y=Mg^{2+}; Ca^{2+}; or Ba^{2+}, *CALPHAD*, **34**:36-44 (2010).

[50] El Guendouzi M., Azougen R., Mounir A., Benbiyi A., Water activities, Osmotic and Activity Coefficients of the System $(NH_4)_2SO_4$–K_2SO_4–H_2O at the Temperature 298.15 K, *CALPHAD*, **27**: 409–414 (2003).

[51] El Guendouzi M., Benbiyi A., Dinane A., Azougen R., Thermodynamic Properties of Multicomponent NaCl–$LiCl$–H_2O Aqueous Solutions at Temperature 298.15 K, *CALPHAD*, **28**: 97–103 (2004).

[52] El Guendouzi M., Benbiyi A., Azougen R., Dinane A., Thermodynamic Properties of Two Ternary Systems {yCsCl+ (1− y) LiCl}(aq) and {yCsCl+ (1− y) NaCl}(aq) at Temperature 298.15 K, *CALPHAD*, **28**: 435–444 (2004).

[53] Marouani M., El Guendouzi M., Determination of Water Activities, Osmotic and Activity Coefficients of the System NH_4NO_3–$LiNO_3$–H_2O at the Temperature 298.15 K, *CALPHAD*, **28**: 321–327 (2004).

[54] Errougui A., El Guendouzi M., Thermodynamic Properties of Ternary Aqueous Mixtures of {yMgCl2+(1− y) Mg (NO3) 2}(aq) at T=298.15 K, *CALPHAD*, **30**: 260–265 (2006).

[55] Archer D.G., Thermodynamic Properties of the $NaNO_3$+H_2O System, *J. Phys. Chem. Ref. Data*, **29**: 1141–1156 (2000).

[56] Patil K.R., Tripathi A.D., Pathak G., Katti S.S., Thermodynamic Properties of Aqueous Electrolyte Solutions. 1. Vapor Pressure of Aqueous Solutions of Lithium Chloride, Lithium Bromide, and Lithium Iodide, *J. Chem. Eng. Data*, **35**: 166-168 (1990).

[57] Archer D.G., Thermodynamic Properties of the KCl+H2O System, *J. Phys. Chem. Ref. Data,* **28**: 1–16 (1999).

[58] Patil K.R., Tripathi A.D., Pathak G., Katti S.S., Thermodynamic Properties of Aqueous Electrolyte Solutions. 2. Vapor Pressure of Aqueous Solutions of Sodium Bromide, Sodium Iodide, Potassium Chloride, Potassium Bromide, Potassium Iodide, Rubidium Chloride, Cesium Chloride, Cesium Bromide, Cesium Iodide, Magnesium Chloride, Calcium Chloride, Calcium Bromide, Calcium Iodide, Strontium Chloride, Strontium Bromide, Strontium Iodide, Barium Chloride, and Barium Bromide, *J. Chem. Eng. Data,* **36**: 225-230 (1991).

[59] Linke W.F., Seidell A., "Solubilities of Inorganic and Metal-Organic Compounds II", American Chemical Society, Washington, (1965).

[60] Hu B., Song P., Li Y., Li W., Solubility Prediction in the Ternary Systems NaCl–RbCl–H_2O, KCl–CsCl–H_2O and KBr–CsBr–H_2O at 25 0C Using the Ion-Interaction Model, *CALPHAD,* **31**: 541–544 (2007).

[61] Brelvi S. W., O'Connell J. P., Corresponding States Correlation for Liquid Compressibility and Partial Molal Volumes of Gases at Infinite Dilution in Liquids, *AIChE J*., **18**: 1239–1243 (1972).

[62] Rumpf B., Nicolaisen H., Öcal C., Maurer G., Solubility of Carbon Dioxide in Aqueous Solutions of Sodium Chloride: Experimental Results and Correlation, *J. Soln. Chem*., **23**: 431-448 (1994).

[63] Austgen D. M., Rochelle G. T., Peng X., Chen C. C., Model of Vapor-Liquid Equilibria for Aqueous Acid Gas-Alkanolamine Systems Using the Electrolyte NRTL Equation, Ind. Eng. Chem. Res., 28:1060–1073 (1989).

[64] Posey M.L., G.T. Rochelle, A Thermodynamic Model of Methyldiethanolamine-CO_2-H_2S-Water, *Ind. Eng. Chem. Res*., **36**: 3944–3953 (1997).

[65] Haghtalab, A., Shojaeian, A., Modeling Solubility of Acid Gases in Alkanolamines Using the Nonelectrolyte Wilson-Nonrandom Factor Model, *Fluid Phase Equilib.,* **289**: 6–14 (2010).

[66] Li Y. G., Mather A. E., Correlation and Prediction of the Solubility of the H_2S and CO_2 Carbon Dioxide in Aqueous Solution of Methyldiethanolamine, *Ind. Eng. Chem. Res.*, **36**: 2760–2765 (1997).

[67] Vahidi M, Matin NS, Goharrokhi M, Jenab MH, Modeling of (vapor+liquid) Equilibrium and Enthalpy of Solution of Carbon Dioxide (CO_2) in Aqueous methyldiethanolamine (MDEA) Solutions, Abdi MA, Najibi SH., Correlation of CO_2 Solubility in N-Methyldiethanolamine+Pi Perazine Aqueous Solutions Using Extended Debye-Hückel Model, *J. Chem. Thermodyn.*, **41**: 1272–1278 (2009).

[68] Arcis H., Rodier L., Ballerat-Busserolles K., Coxam J.-Y., J. Chem. Thermodyn., 41:783–789 (2009).

[69] Chunxi L., Fürst W., Representation of CO_2 and H_2S Solubility in Aqueous MDEA Solutions Using an Electrolyte Equation of state, *Chem. Eng. Sci.,* **55**: 2975–2988 (2000).

[70] Derks P. W. J., Hogendoorn J. A., Versteeg G. F., Experimental and Theoretical Study of the Solubility of Carbon Dioxide in Aqueous Blends of Piperazine and N-methyldiethanolamine, *J. Chem. Thermodyn*., **42**: 151–163 (2010).

[71] Maddox R.N., Bhairi A.H., Diers J.R., "Research Report RR-104", Gas Processors Association, Tulsa, (1987).

[72] Jou F. Y., Mather A. E., Otto F. D., Solubility of H_2S and CO_2 in Aqueous Methyldiethanolamine Solutions, *Ind. Eng. Chem. Process Des. Dev.,* **21**: 539–544 (1982).

[73] MacGregor R.J., Mather A.E., Equilibrium Solubility of H_2S and CO_2 and their Mixtures in a Mixed Solvent, *Can. J. Chem. Eng*., **69**: 1357–1366 (1991).

[74] Austgen D. M., Rochelle G. T., Chen C. C., Model of Vapor-Liquid Equilibria for Aqueous Acid Gas-Alkanolamine Systems. 2. Representation of H_2S and CO_2 Solubility in Aqueous MDEA and CO_2 Solubility in Aqueous Mixtures of MDEA with MEA or DEA, *Ind. Eng. Chem. Res.,* **30**:543–555 (1991).

[75] Jou F.-Y., Otto F. D., Mather A. E., Vapor-Liquid Equilibrium of Carbon Dioxide in Aqueous Mixtures of Monoethanolamine and Methyldiethanolamine, *Ind. Eng. Chem. Res.,* **33**: 2002–2005 (1994).

[76] Jou F.-Y., Carroll J.J., Mather A.E., Otto F.D., The Solubility of Carbon Dioxide and Hydrogen Sulfide in a 35 wt% Aqueous Solution of Methyldiethanolamine, *Can. J. Chem. Eng.,* **71**: 264-268 (1993).

[77] Ho B.S., Eguren R.R., Solubility of Acidic Gases in Aqueous DEA and MDEA Solutions. Amoco Production Company, Paper No. 69-a, Presented at "*The 1988 Spring National Meeting of the American Institute of Chemical Engineers",* March 6–10, (1988).